Preparation of Chromium doped uranium nitride via Sol-Gel and Carbothermic reduction

Citation for the original published paper (version of record):
Gonzalez Fonseca, L., Král, J., Hedberg, M. et al (2023). Preparation of Chromium doped uranium nitride via Sol-Gel and Carbothermic reduction. Journal of Nuclear Materials, 574.
http://dx.doi.org/10.1016/j.jnucmat.2022.154190

Journal of Nuclear Materials 574 (2023) 154190

Contents lists available at ScienceDirect

Journal of Nuclear Materials

journal homepage: www.elsevier.com/locate/jnucmat

Nuclear fuels and materials

Preparation of Chromium doped uranium nitride via Sol-Gel and Carbothermic reduction

L.G. Gonzalez Fonseca [a,*], J. Král [b], M. Hedberg [a], T. Retegan Vollmer [a]

[a] Division of Nuclear Chemistry and Industrial Materials Recycling, Department of Chemistry and Chemical Engineering, Chalmers University of Technology. 412 96, Gothenburg, Sweden
[b] Department of Nuclear Chemistry, Faculty of Nuclear Sciences and Physical Engineering, Czech Technical University. 115 19, Prague, Czech Republic

ARTICLE INFO

Article history:
Received 30 August 2022
Revised 14 November 2022
Accepted 5 December 2022
Available online 7 December 2022

Keywords:
Uranium nitride
Chromium precipitations
Ternary phase
U_2CrN_3
Solubility
Microsphere

ABSTRACT

Uranium nitride (UN) has been proposed as an accident tolerant fuel due to its enhanced thermal properties compared to the standard UO_2. However, due to its low oxidation resistance, its implementation in water cooled reactors has not been allowed. A method to improve the corrosion resistance involves doping with oxide scale forming elements such as aluminum or chromium. In this work, UN microspheres were produced by an internal gelation method followed by carbothermic reduction and nitridation. Chromium was added as dopant in the solution to produce a homogenous mixture with uranium. The ternary phase (U_2CrN_3) was observed for the first time in Cr-doped UN microspheres produced via sol-gel and carbothermic reduction. Materials with and without the ternary phase were produced, and a mechanism of reaction was proposed.

Chromium precipitations were also observed on the surface of the microspheres produced, indicating low solubility of Cr compounds in the UN matrix. ICP-MS and XRF measurements showed that Cr content is reduced after heating treatments, probably due to evaporation. Additionally, these results showed that Cr in the ternary phase is completely soluble in aqua regia, unlike the Cr in the material without the ternary phase.

1. Introduction

Advance technology fuels or accident tolerant fuels (ATF) are nuclear fuels that are designed to reduce the probability of accidents and improve the safety of the fuel under severe accident conditions. This could be achieved by modifying the fuel and the cladding currently used in the industry. So far, changes in the claddings have been studied in more depth as it is the first barrier between the environment and the radioactive fuel and fission products [1]. However, the use of these modified claddings negatively impacts the neutronics in the reactor, reducing the efficiency of the fuel [2,3]. This problem could be overcome by, for example, increasing the enrichment of the uranium oxide or increasing the uranium density in the fuel [2]. The latter has been observed in other uranium compounds such as uranium carbides, silicides, and nitrides [4]. Amongst them, uranium nitride (UN) is considered a promising fuel due to its improved thermal properties and similar melting point compared to the standard UO_2 [5]. One major drawback in using UN fuel is that it is unstable in oxidizing environments [6]. The reaction with oxygen, water or steam causes the loss of structural integrity, resulting in the disintegration and pulverization of fuel pellets [7,8].

Different methods to aid the corrosion resistance of UN have been mentioned before [9–12]. The general concept is to mix the uranium nitride with a material that can protect it if the fuel comes into contact with air or water. Oxide scale forming elements such as aluminum and chromium could provide sufficient protection to slow down the oxidation of UN in the case of an accident [13]. A screening study on possible dopants for UN showed that chromium seems to increase the survivability of UN pellets in boiling water [14]. However, the data presented was limited. Chromium doping of UN has been studied further using powder methods to mix UN and CrN [13,15].

This work is intended to expand the research on chromium as a dopant for the possible use of UN fuel in LWR. Chromium-doped UN in the shape of microspheres was fabricated via a sol-gel process combined with carbothermic reduction in a nitrogen atmosphere. The dissolution of CrN in the UN matrix was studied using

---

[*] Corresponding author.
E-mail address: luisg@chalmers.se (L.G. Gonzalez Fonseca).

https://doi.org/10.1016/j.jnucmat.2022.154190

X-ray diffraction analysis (XRD) and scanning electron microscopy (SEM). Moreover, the effect of different levels of chromium doping on manufacturing and properties of UN was investigated.

2. Theory

2.1. The uranium-chromium-nitrogen system

The uranium and nitrogen system has been defined before [16], and three phases have been identified. Uranium mononitride (UN) exists as an FCC structure of NaCl with a lattice parameter of 0.4890 nm. Uranium dinitride (UN_2) is found as an FFC structure of CaF_2 and a lattice parameter of 0.5310 nm. Uranium sesquinitride (U_2N_3) is found in two different phases, an α-U_2N_3 with an Ia-3 structure with lattice parameter of 1.0699 nm and a trigonal structure with a lattice parameter of a/b = 0.3693 nm and c = 0.5770 nm. Solid solutions of UN_2 and α-U_2N_3 are stable at all intermediate compositions above N/U=1.54 [17], and will be referred as $UN_{1.5+x}$ in this study. The phase diagram for the U-N system published by Matthews et al. [16] can be used to determine the temperatures at which such phases are stable. Higher nitrides can be denitrided back into the mononitride at temperatures above 1473 K in an inert atmosphere. In the Cr-N system only two phases have been observed: Chromium mononitride (FCC-NaCl, a=0.4150 nm) and dichromium nitride (hexagonal-V_2N, a=0.478 nm, c=0.441 nm).

The U-Cr-N ternary system was previously investigated by Holleck et al. [18]. They concluded that at temperatures between 1473 and 1873 K chromium replaces the uranium in the crystal structure. However, the decrease in bond length limits the amounts of U that can be replaced by Cr to 33 at-%. The nitride structure formed is therefore a ternary phase with the stochiometric formula U_2CrN_3. This phase is present in an orthorhombic crystal structure and belongs to the space group Immm [19]. Theoretical calculations made by Mishchenko et al. [13] have shown that the solubility of CrN in UN crystal is thermodynamically favorable and expected.

3. Experimental

3.1. Chemicals

Uranyl nitrate hexahydrate (UNH) [$UO_2(NO_3)_2$•$6H_2O$] was prepared inhouse by dissolving metallic uranium (in the form of a metal rod) with conc. HNO_3. The precipitated UNH crystals were filtered and dried in air. Solutions of uranyl nitrate were prepared by dissolving UNH crystals in ultra-pure water (18.2 MΩ•cm). Chromium nitrate [$Cr(NO_3)_3$•$9H_2O$] (Sigma-Aldrich, 99%) was used as the chromium source.

Carbon black (MOGUL L) provided by CABOT was used as a carbon source. Hexamethylenetetramine (HMTA) 99% purity was provided by Sigma Aldrich and was used as the gelation agent. Urea in solid form with 99% purity was also provided by Sigma Aldrich. Laboratory grade Triton X-100 was received from Sigma Aldrich and used as a non-ionic surfactant to disperse the carbon powder in the solution [20]. Ultra-pure water (18.2 MΩ•cm) was used for all aqueous dilutions.

Silicone oil v 1000 from Rhodorsil was used as the gelation medium. Petroleum ether from Alfa-Aesar was used to wash the oil from the spheres, while ammonium hydroxide solution 28-30% from Sigma-Aldrich was used to wash the unreacted chemicals and age the spheres.

3.2. Methods

3.2.1. Synthesis of UN and (U,Cr)N microspheres

The Sol-Gel process was performed by slowly dripping a cool solution into a hot oil. Firstly, 10 or 15 mL batches with 1.5 M solutions of $UO_2(NO_3)_2$ were cooled in a double jacketed beaker connected to a water bath at 277 K. The NO_3^-/UO_2^{2+} ratio was kept at 2 to avoid the use of two sources of uranium. Chromium was added as a dopant in metal molar fractions of 0.05, 0.1 or 0.2. $Cr(NO_3)_3$•$9H_2O$ in solid form was dissolved in the uranyl solution to reach the desired molar fraction. Solid urea was added to reach a molar ratio of 1.3 between urea and total metal. After the urea was completely dissolved, HMTA was added slowly to reach a molar ratio of 1.8 with the metal. Triton X-100 was added to reach a concentration of 0.02 g/mL. Once the mixture was homogeneous, graphite was added to obtain a 2.5 molar ratio C/Metal. The sol was then left to completely mix for 10-15 minutes. The final metal concentration was estimated to be 1.2 M for materials with high chromium doping. The parameters and ratios used were found experimentally to produce good quality microspheres.

Solutions were then manually dropped into the gelation medium (silicon oil at 363 K), attempting to maintain a similar droplet size. The spheres were allowed to form and fall into the 30 cm long column. On average, the process took two minutes per milliliter of solution. Spheres were collected and washed twice for 10 minutes with petroleum ether to remove the silicone oil. The spheres were then washed in concentrated ammonia solution for 10 minutes to remove unreacted compounds. Washing with diluted ammonia solution was performed to age the spheres. The last step was to leave the spheres to air dry for one or two days.

The dried material was placed in an alumina crucible and taken into an alumina tube furnace ETF 30-50/18-S with a maximum operating temperature of 2073 K. Two different heating profiles were used during the nitridation process to produce different types of chromium doped UN. They are summarized in Figure 1. In profile A, a drying and reducing step was done previous to the nitridation process to reduce the cracking of the spheres. The nitridation temperature was set at 1823 K with an hour of decarburization at 1923 K. Heating and dwelling were performed in a mixed atmosphere gas (5% H_2 and 95% N_2). The cooling was done in an argon atmosphere to avoid the formation of hyperstoichiometric nitrides (UN_2 and U_2N_3). The drying and nitridation steps were combined in profile B, and the maximal temperature was changed to 1773 K. Two different cooling gases were used: argon or the same mixed atmosphere (H_2/N_2).

Denitridation of samples containing higher nitrides was done by heating the samples to 1200 K with a heating rate of 10 K/min. The samples remain at the maximal temperature for two hours under an argon atmosphere. Afterwards, the furnace was cooled down with a cooling rate of 10 K/min.

Surface structure and elemental distribution were examined using a Hitachi TM 3000 tabletop SEM/EDX. Part of the material was ground, and the phases and crystallographic structure of the powders were investigated by X-ray diffraction (XRD) using a BRUKER D2 PHASER XRD which includes monochromatic Cu (λ = 0.154184 nm) radiation source in 2θ range of 20° - 144° and a lynxeye detector. The operation voltage and current used are, respectively, 30 kV and 10 mA. The lattice parameters were calculated from the XRD peaks using Rietveld refinement.

The elemental composition was determined using a LECO CS744 instrument for carbon, and a LECO TC-436DR for nitrogen and oxygen. Two methods were used to evaluate the chromium/uranium ratio in the materials synthesized: A Thermo-Fisher inductively coupled plasma mass spectrometer (ICP-MS) and an XRF instrument (Delta-50, Innov-X, Olympus).

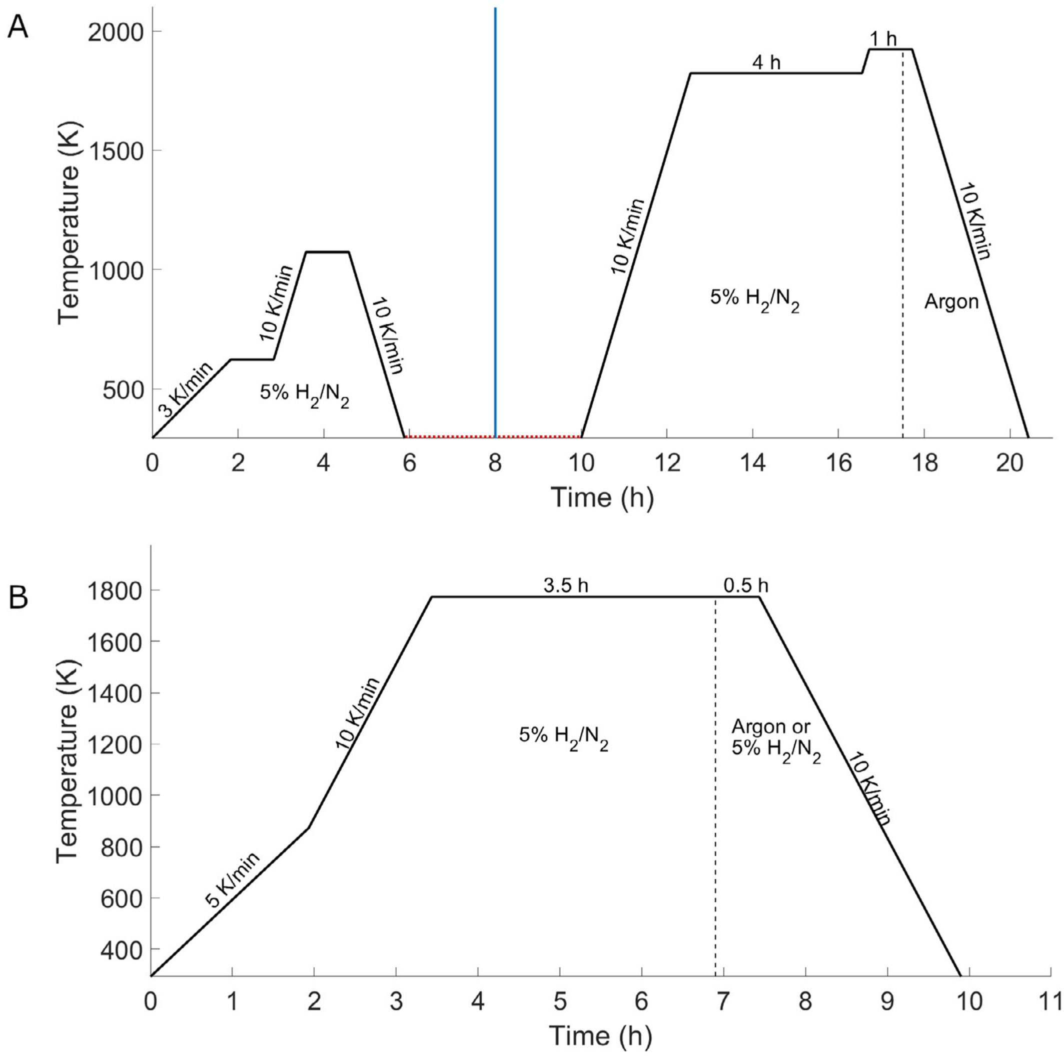

Figure 1. Temperature profile for carbothermic reduction of uranium nitride. A) two different heating steps for reduction and nitridation of the materials. Max. temperature of 1923 K and cooling down in Ar gas. B) one heating step nitridation process at max. temperature of 1773 K. Cooling down in either Ar gas or 5% H_2/N_2.

Microsphere's density was calculated by measuring the average weight of the spheres and using a light microscope to estimate the average sphere diameter.

4. Results

Chromium doped UN microspheres were produced using the different heating profiles. In this section, a summary of the main results will be presented. The results will focus on the surface microstructure, phases formed and elemental composition.

4.1. UN and (U,Cr)N using heating profile A

A series of analyses, such as elemental analysis and XRD measurements, were made to evaluate the properties of the materials produced. Firstly, the elemental composition was measured. Average values for carbon, nitrogen, and oxygen are listed in Table 1. Carbon and oxygen were present in all samples as impurities. Carbon contents between 0.01 and 1.7 wt-% were measured, while oxygen impurities varied between 0.13 and 0.6 wt-%. Different batches with the same composition were made to observe the repetitibility of the process. Batch U95CrN-3 and U80Cr20N-3 were produced in a smaller volume batch (10 mL).

Figure 2 shows the XRD patterns of the UN microspheres with different expected ratios of chromium. The pure UN diffractogam was simulated using the crystal structure and the powder cell (version 2.4) software. The lattice parameter for the U95Cr5N-2, U90Cr10N-1 and U80Cr20N-1 were measured to be 0.4916 nm, 0.4909 nm, and 0.4901 nm, respectively.

SEM analysis (Figure 3) showed the presence of a phase precipitation in the surface of the microspheres. The phase was identified as a chromium rich phase. However, such phase was not present in the XRD patterns.

The chromium content of the samples in Table 1 was measured at different stages during the synthesis of (U,Cr)N: in the as-produced spheres, after reduction to UO_2 at 1073 K and after nitridation at 1923 K. Cr-doped UN microspheres were dissolved in aqua regia at room temperature for 12 hours. The solutions were then filtered and measured using ICP-MS, and the results obtained are summarized in Table 2.

As can be seen, the Chromium content is partially reduced after the reduction step at 1073 K. After nitridation at 1923 K the chromium content was further reduced, and to a greater extent. For example, the chromium mol ratio with uranium was reduced from 14.6 mol-% in the as-produced microspheres to 9.6 mol-% after reduction and to 2.5 mol-% after the nitridation.

Table 1
Elemental analysis and density of synthesized Cr-doped UN micropsheres using heating profile A. Uncertainties calculated by measuring triplicates.

Sample name	Carbon content (wt-%)	Nitrogen content (wt-%)	Oxygen content (wt-%)	Microsphere density (g/cm^3)
UN-1	0.011 ± 0.004	5.4 ± 0.3	0.3 ± 0.2	4.16 ± 0.06
U95Cr5N-1	1.1 ± 0.1	4.4 ± 0.1	0.16 ± 0.02	3.26 ± 0.09
U95Cr5N-2	1.2 ± 0.4	3.92 ± 0.02	0.15 ± 0.01	3.6 ± 0.1
U95Cr5N-3	0.01 ± 0.01	5.55 ± 0.04	0.54 ± 0.03	3.4 ± 0.1
U90Cr10N-1	1.0 ± 0.4	4.31 ± 0.01	0.13 ± 0.01	3.7 ± 0.2
U90Cr10N-2	1.7 ± 0.2	4.5 ± 0.2	0.21 ± 0.02	3.83 ± 0.07
U80Cr20N-1	0.66 ± 0.04	4.77 ± 0.07	0.17 ± 0.02	4.55 ± 0.05
U80Cr20N-2	1.11 ± 0.03	4.65	0.14	5.00 ± 0.06
U80Cr20N-3	0.79 ± 0.04	4.65 ± 0.02	0.23 ± 0.01	3.96 ± 0.04

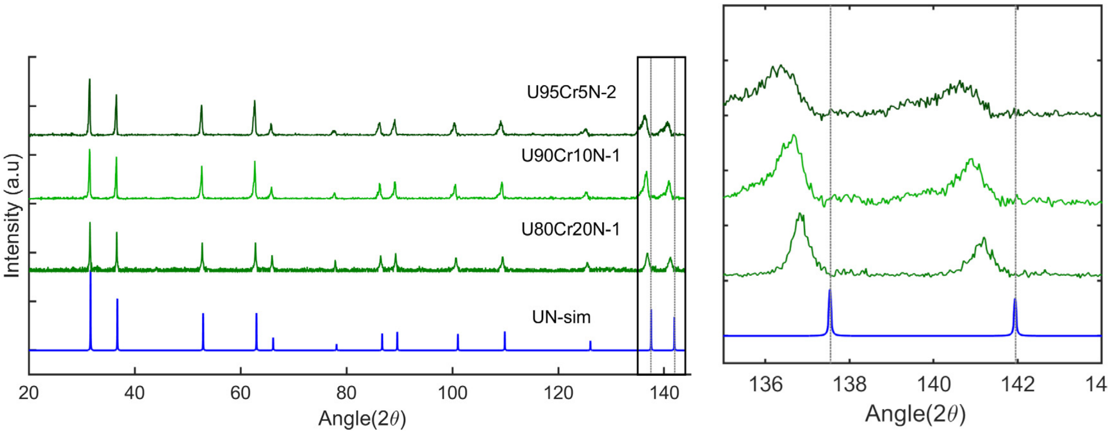

Figure 2. X-ray difractograms for UN spheres doped with different levels of Cr and synthesized using heating profile A, compared to a simulated XRD pattern of pure UN. The lattice parameter for the 5%, 10% and 20% Cr mol-% were measured to be 0.4916 nm, 0.4909 nm, and 0.4901 nm, respectively. The lattice parameter used for the simulated UN was 0.489nm.

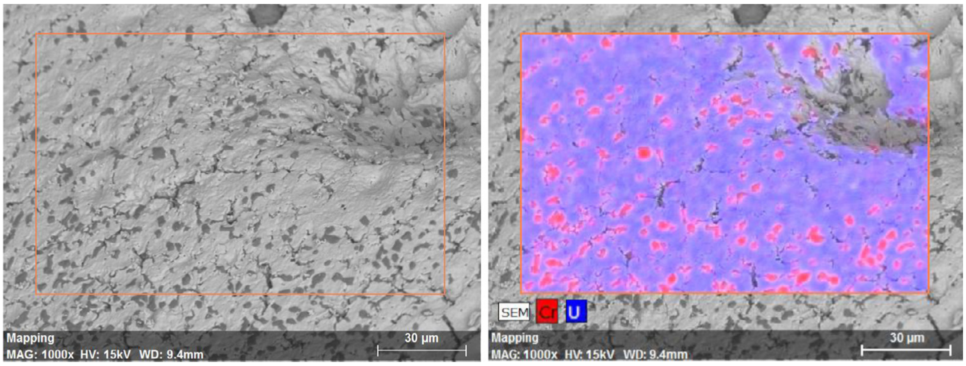

Figure 3. SEM image of the surface of a U80Cr20N-1 microsphere after synthesis using profile A. The Cr (red) and U (blue) mapping is presented on the right to show the precipitation of a chromium rich phase.

4.2. Production of Cr-doped uranium nitrides at lower temperatures

To better understand the chromium losses, microspheres with 20 mol-% Cr content were produced and heated to different temperatures using the heating profile B (Figure 1). The cooling gas used was the same gas mixture used during the reaction (5% H_2/N_2). The reaction progress was followed using the elemental analysis of the products, listed in Table 3. As observed, the nitridation starts at 1473 K, but temperatures of 1773 K are necessary to reduce the carbon and oxygen concentrations to levels below 1 wt-%.

The XRD patterns of the products can be seen in Figure 4. Uranium nitrides were observed after 1473 K. Uranium oxides were not visible after 1673 K. At this temperature, the ternary phase was also present in the products for the first time.

Surface microscopy of microspheres heated to different temperatures can be seen in Figure 5. The microstructure of the sphere seems to also change depending on the maximal temperature for reaction. At 1273 K there are lumps of carbon spread on the surface. Once the temperature reaches 1473 K, the carbon seems to diminish, and a darker phase seems to appear on the surface (marked with circles in Figure 5). At 1673 K the carbon spots are almost eliminated, and if cooled down in H_2/N_2 atmosphere, the Cr rich phase precipitates are not observed. If temperature is increased up to 1773 K, the porosity seems to increase on the surface, probably due to CrN decomposition/evaporation.

The microspheres were also heated with the heating profile B, but the cooling atmosphere was changed to Ar to prevent the formation of hyperstoichiometric nitrides. As seen in Figure 6, the Cr rich phase precipitations were seen again on the surface of the spheres. Moreover, a closer look at the microsphere sur-

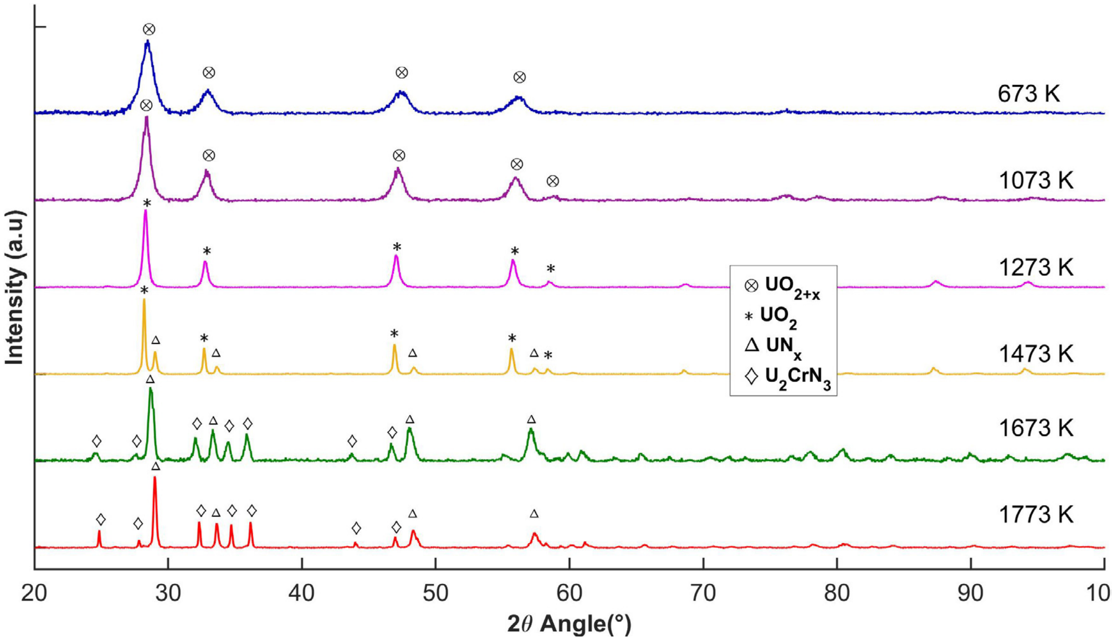

Figure 4. XRD patterns measured for the materials heated up to different temperatures and cooled down in the synthesis gas (H_2/N_2). Phases present were: UO$_{2+x}$ (⊗), UO$_2$ (∗), UN$_{1.5+x}$ (Δ), U$_2$CrN$_3$ (◇).

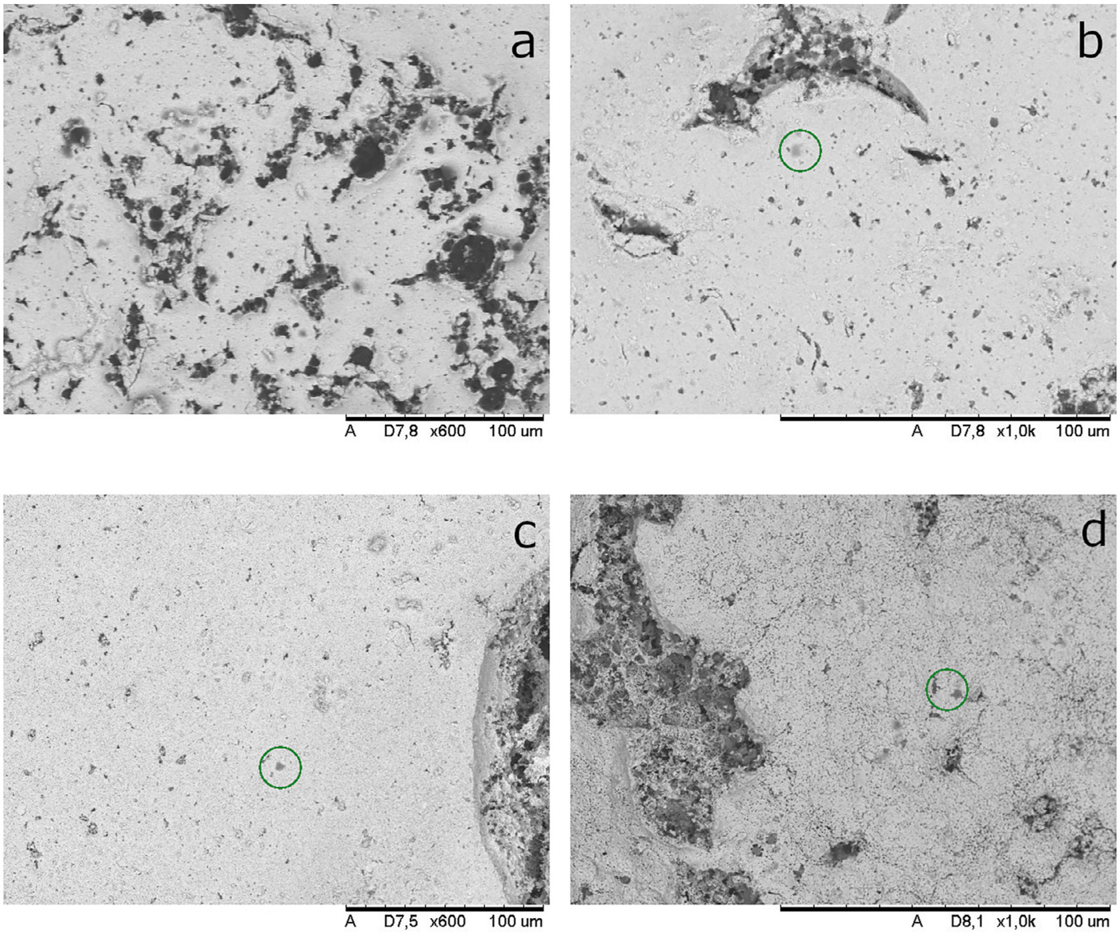

Figure 5. SEM images of microspheres' surface after reaction at a) 1273 K, b) 1473 K, c) 1673 K, and d) 1773 K using heating profile B. The material was cooled down in the synthesis gas (H_2/N_2). A secondary darker phase is signalized with a green circle.

Table 2
Chromium content (in molar metal fraction) of the materials at different intervals during the heating profile A, measured using ICP-MS. n.d. stands for not determined. Uncertainties calculated by measuring triplicates.

Sample name	Expected Cr content (mol-%)	Cr content as-produced (mol-%)	Cr content after reduction (mol-%)	Cr content after nitridation (mol-%)
U95Cr5N-1	5	5.8 ± 0.6	7.8 ± 0.7	1.0 ± 0.4
U95Cr5N-2	5	5.5 ± 0.5	5.5 ± 0.7	1.0 ± 0.4
U95Cr5N-3	5	n.d.	6.1 ± 0.9	2.5 ± 0.3
U90Cr10N-1	10	11.2 ± 0.9	7.0 ± 0.7	4.1 ± 0.4
U90Cr10N-2	10	15 ± 1	9.6 ± 0.6	2.5 ±0.4
U80Cr20N-1	20	22 ± 1	20 ± 1	4.9 ± 0.7
U80Cr20N-2	20	26 ± 1	19 ± 1	n.d.
U80Cr20N-3	20	18.4 ± 0.8	12 ± 1	4.6 ± 0.6

Table 3
Elemental analysis of Cr-doped UN micropspheres after heating up to different temperatures in 5% H_2/N_2 and cooled down in the same gas. Chromium content was measured using ICP-MS with an expected chromium molar metal fraction of 20% for all the samples. Uncertainties calculated by measuring triplicates. n.d. stands for not determined.

Dwelling Temperature (K)	Carbon content (wt-%)	Nitrogen content (wt-%)	Oxygen content (wt-%)	Cr content after reaction (mol-%)	Microsphere density (g/cm^3)	Lattice parameter of $UN_{1.5+x}$ (nm)
As-produced	14.1 ± 0.5	n.d.	n.d.	20 ± 2	1.78 ± 0.06	-
673	11.4 ± 0.1	0.89 ± 0.02	10.7 ± 0.3	19 ± 1	n.d.	-
1073	10.2 ± 0.3	0.110 ± 0.004	10.1 ± 0.3	10 ± 1	n.d.	-
1273	10.0 ± 0.2	0.10 ± 0.01	8.8 ± 0.9	9 ± 1	2.55 ± 0.02	-
1473	7.7 ± 0.1	2.34 ± 0.01	6.2 ± 0.1	4.9 ± 0.3	4.41 ± 0.01	1.061
1673	1.1 ± 0.1	8.11 ± 0.04	0.42 ± 0.01	19 ± 1	5.57 ± 0.05	1.065
1773	0.036 ± 0.001	8.277 ± 0.004	0.25 ± 0.01	19 ± 2	5.42 ± 0.01	1.064

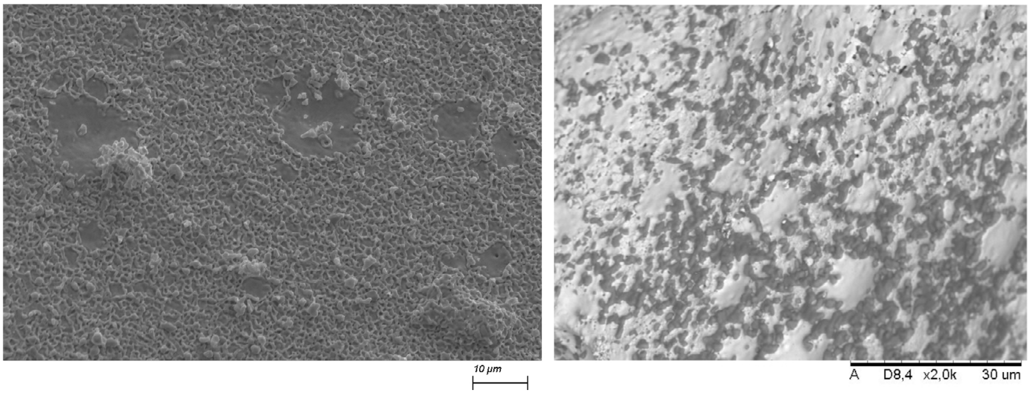

Figure 6. SEM image of the surface of the Cr-doped UN microsphere showing the precipitation of a pebble like chromium rich phase (black) on most of the surface after synthesis using argon as the cooling gas.

Table 4
Elemental analysis of Cr-doped UN micropspheres after synthesis using different cooling atmospheres and dwelling temperatures. Chromium content was measured using ICP-MS. An expected chromium molar metal fraction of 20% for all the samples. Uncertainties calculated by measuring triplicates.

Temperature (K)	Cooling atmosphere	Carbon content (wt-%)	Nitrogen content (wt-%)	Oxygen content (wt-%)	Cr content after nitridation (mol-%)
1923	Ar	0.66 ± 0.04	4.77 ± 0.07	0.17 ± 0.02	4.9 ± 0.7
1773	Ar	1.36	4.42	0.29	2 ± 2
1773	5% H_2 / N_2	0.036 ± 0.001	8.277 ± 0.004	0.25 ± 0.01	19 ± 2

face showed that this phase seems to cover the entirety of the surface.

A comparison of the elemental analysis and XRD of Cr-doped microspheres after heating treatment can be found in Table 4 and Figure 7, respectively.

The chromium content ratio in the microspheres was also measured using X-ray fluorescence (XRF) to confirm the results from the ICP-MS. The Cr molar metal ratio was determined, and results are listed in Table 5. Each sample represents a batch produced using the same conditions, and results are presented to observe the repeatability of the synthesis and the XRF equipment. As can be seen, the chromium content varied between 17.5 and 23.7 mol-%. The expected chromium content was 20 mol-%. After cooling down in Ar, Cr content was always lower than samples cooled down in H_2/N_2.

4.3. Production of UN combined with U_2CrN_3

Up to this point, the production of the ternary phase has only been observed in combination with $UN_{1.5+x}$. The next step in the process was to reduce the samples back to UN. This denitridation was achieved by reheating the samples to 1473 K in an argon atmosphere for 2 hours. For example, denitridation of sample UCrN-1 can be followed in the XRD patterns in Figure 8. The phase composition was calculated using Rietveld refinement. The compositions obtained for the U_2CrN_3 and $UN_{1.5+x}$ were 20.8% and 79.2%, respectively. After denitridation, the compositions for U_2CrN_3 and UN were 21.5% and 78.5%, respectively.

The microscopy of spheres after denitridation can be seen in Figure 9. The ternary phase relocated to form patches in the sur-

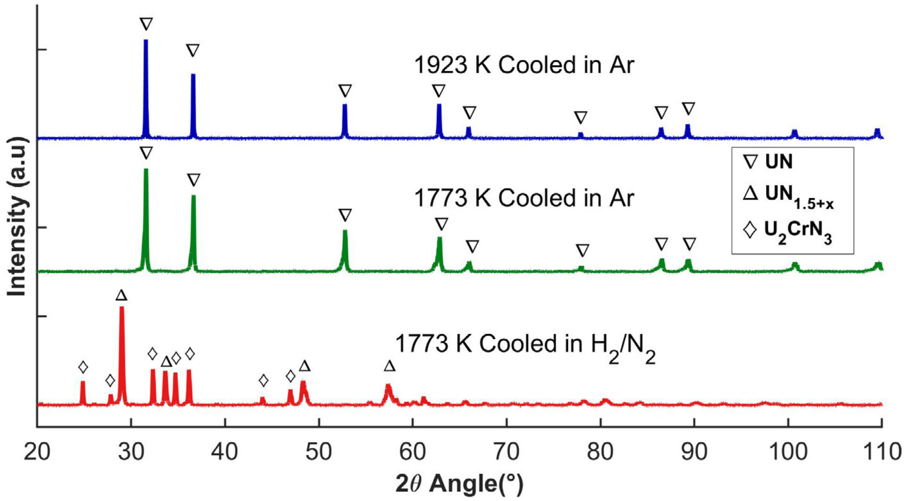

Figure 7. XRD patterns of Cr-doped UN micropsheres after synthesis using different cooling atmospheres and dwelling temperatures. The final phases present are UN (∇), $UN_{1.5+x}$ (Δ), and U_2CrN_3 (◊).

Table 5
Chromium content measured using x-ray fluorescence (XRF) in the microspheres synthesized at 1773 K using H_2/N_2 or Ar as cooling atmospheres. An expected chromium molar metal of 20 mol-% was expected for all the samples. n.d. stands for not determined.

Sample	Chromium content before reaction (mol-%)	Cr content after reaction and cooling down in H_2/N_2 (mol-%)	Cr content after reaction and cooling down in Ar (mol-%)
UCrN-1	21.0 ± 0.1	18.8 ± 0.1	n.d.
UCrN-2	21.1 ± 0.1	21.3 ± 0.3	20.0 ± 0.1
UCrN-3	20.5 ± 0.1	23.7 ± 0.2	22 ± 1
UCrN-4	20.6 ± 0.1	19.2 ± 0.5	17.5 ± 0.1

face of the spheres. When closer examined, it seems that such spots are positioned near small surface cracks.

5. Discussion

5.1. UN and (U,Cr)N using heating profile A

The higher carbon content compared to un-doped materials [21] can be explained by the lower theoretical amount of carbon needed for the Cr to react with respect to the uranium. Additionally, a higher amount of organic chemicals was used to be able to precipitate the chromium containing solutions. However, samples with higher carbon content showed lower oxygen in the samples. Cracking was observed in all Cr-doped UN microspheres. The cracking was attributed to the increase in the HMTA/metal ratio required to gelate the doped uranium microspheres.

The lack of other peaks in the XRDs in Figure 2 indicates that new uranium phases, such as carbides or higher nitrides, were not formed after reaction. Carbon measured is mainly present as uranium carbide dissolved in the UN forming a $UC_xN_{1\text{-}x}$ phase. The replacement of nitrogen by carbon in the crystal structure can explain the displacement of the peaks towards smaller angles and the increase in the calculated lattice parameter. Additionally, materials with higher chromium doping appear to shift the peaks towards higher angles. However it is not possible to determine the combined effect of both C and Cr in the lattice parameters, as carbon would increase the lattice and chromium will decrease it. The ternary phase (U_2CrN_3) mentioned in the theory section was not observed in these XRD patterns. Similar results were previously found by Herman et al. [14]. However, this behavior is unexpected as the phase is supposed to be thermodynamically stable up to 1873 K, according to Mishchenko et al. [13]. This suggests that the phase was never formed in the synthesized materials or that it was not stable during reaction.

The presence of a chromium containing phase in the SEM (Figure 3) which is not seen in the XRDs suggests a much lower quantity of that phase in comparison with UN. Elemental mapping also showed that the phase does not contain uranium. This means that the black spots are a phase of either metallic chromium, chromium nitride, carbide, or oxide. More importantly this indicates that there is a low solubility of the chromium in the UN phase.

A pink coloration of the alumina boat where the samples were nitrided was observed after the nitridation process. The coloration was explained by the formation of a $AlCrO_3$ compound, probably due to vaporization of chromium at high temperatures. Chromium loss during the reduction process (Table 2) could be explained by the evaporation of a $CrO_2(OH)_2$ species which can occur at temperatures as low as 873 K [22,23]. However, the conditions for the production of this phase are not likely to exist in the system. Pure chromium nitride is unstable at temperatures above 1673 K, where it decomposes into Cr_2N, which then decomposes into metallic chromium [24,25]. Simultaneously, Cr can be volatilized due to its vapor pressure at these temperatures [26].

5.2. Production of Cr-doped uranium nitrides using heating profile B

The nitrogen content in the spheres after reaction was summarized in Table 3. It is firstly reduced due to the elimination of unwashed organic reactants. It was observed in Figure 4 that uranium nitride phases were first observed in the samples heated at 1473 K. At 1673 K the UO_2 signals had disappeared; additionally, the peaks for the existing nitride phases are shifted towards lower angles (increase in lattice parameters) probably due to high carbon

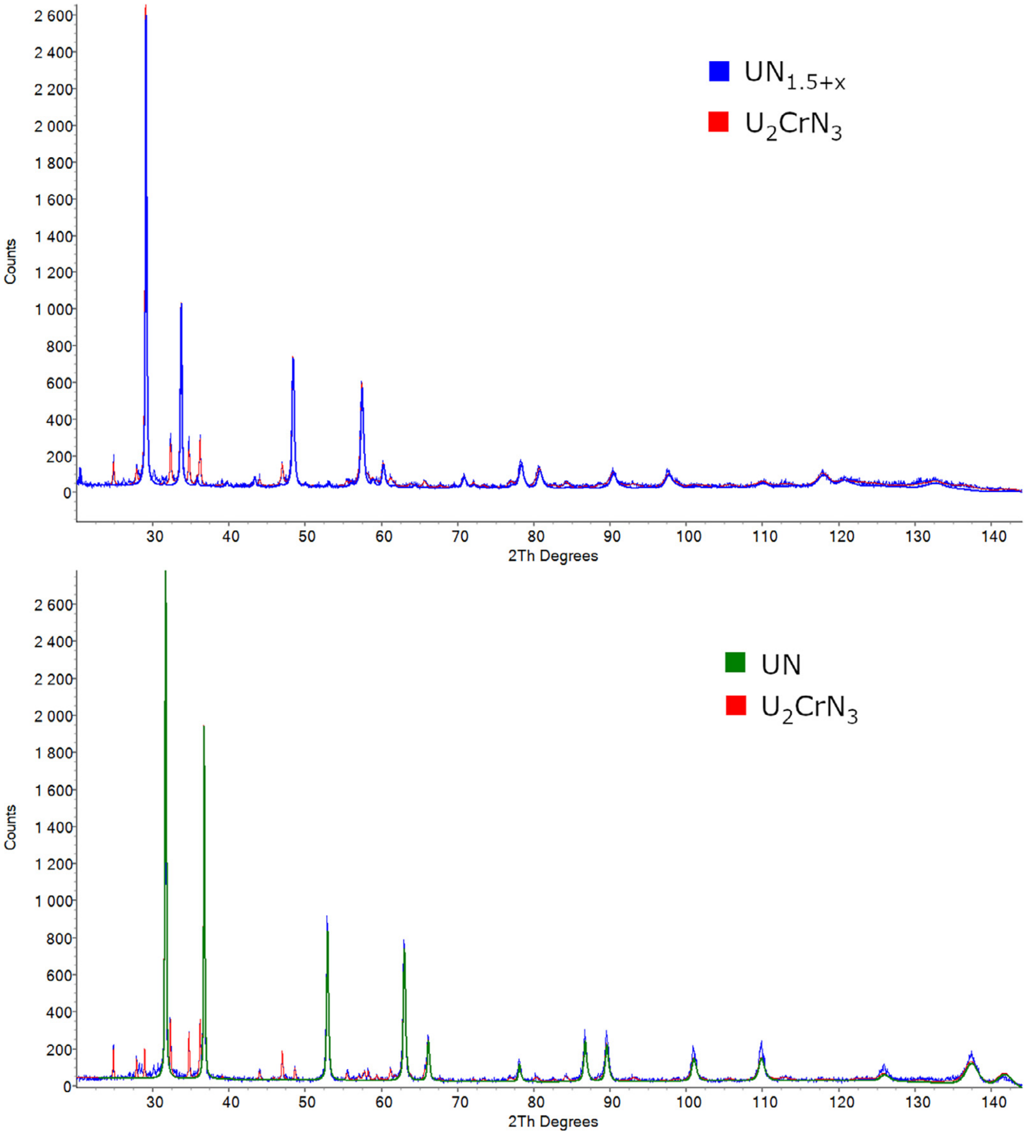

Figure 8. XRD patterns of UCrN-1 microspheres before (upper) and after (lower) denitridation showing the transformation of the $UN_{1.5+x}$ phase (blue) into the UN phase (green). The ternary phase was indicated in both patters in a red color.

impurities left after the reaction. At 1773 K the carbon content is reduced further, and the peaks are found in the expected angles for the pure phases. The nitrogen content measured in the sample heated at 1773 K was 8.277 wt-%, which is achieved if all Cr is in the U_2CrN_3 phase, and the remaining uranium is an approximately 50-50% solid solution of U_2N_3 and UN_2. This was later confirmed using XRD (Figure 4), where the lattice parameter of the α-U_2N_3 phase was calculated using Rietveld refinement to be 1.064 nm, which can be related to a N/U ratio of about 1.75 [17]. Therefore, the solid solution of nitride phases was referred as $UN_{1.5+x}$ in this study. The refinement also showed that the composition of the phases was 46.6% and 53.4% for U_2CrN_3 and $UN_{1.5+x}$, respectively. The ternary phase composition calculated was lower than the expected composition of 52% and 48% for U_2CrN_3 and $UN_{1.5+x}$, respectively. The difference can be due to errors in the refinement, or if some of the Cr was not present in the form of U_2CrN_3 phase.

It can be observed in Table 4 that the carbothermic reduction completion was similar regardless of temperature of reaction or cooling down gas as the oxygen content was lowered to similar levels (0.17-0.29 wt-%). However, the decarburization was not finished in samples cooled down in argon. Similarly the final carbon content is also increased if decarbonization at 1923 K is avoided entirely. Higher nitrogen content in the samples cooled down in H_2/N_2 is explained by the presence of the $UN_{1.5+x}$ phase and the higher nitrogen ratio in the ternary phase U_2CrN_3.

The chromium content measured by ICP-MS (Table 4) was below 5 mol-% for samples cooled down in Ar, but almost no change was detected in the sample cooled down in H_2/N_2 with respect to the expected value (20 mol-%). This and the presence of the Cr rich phase on the surface of spheres cooled down in Ar leads to the following assumptions:

- As the nitrogen content is low, the Cr rich phase is most likely metallic Cr. Chromium carbides are another possible species, but at the reaction temperatures such phases should have reacted and transformed into nitrides and then decompose. [25,27,28]
- Part of this chromium reacts with the aqua regia, but a protective layer is formed around the Cr. The oxide surface is no longer soluble in the aqua regia, and therefore is not quantitatively measured in the ICP-MS [29].

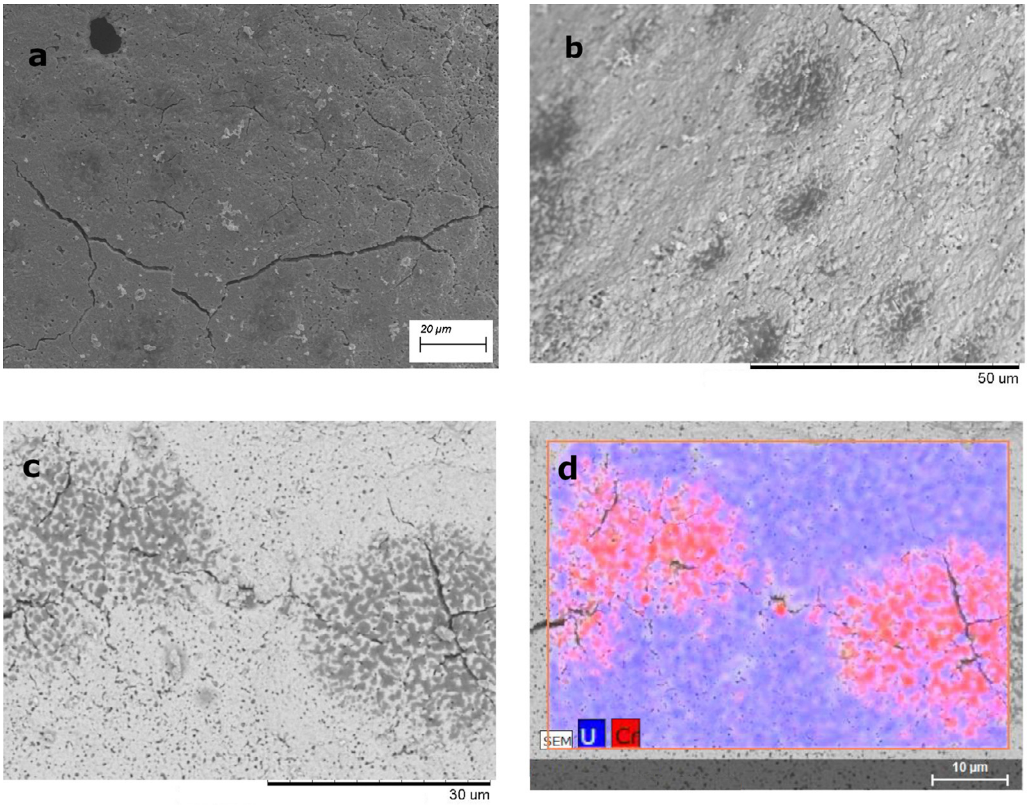

Figure 9. Chromium (red) and uranium (blue) distribution on the SEM image of the UCrN-1 microsphere after denitridation, showing the presence of the U_2CrN_3 phase on the surface of the sphere.

XRF measurements (Table 5) showed that Cr content is similar for samples cooled down in Ar or H_2/N_2. Moreover, it confirmed the assumption that chromium in the Ar-cooled UN spheres is present in a phase that is not completely soluble in the aqua regia. On the other hand, the results also showed that the ternary phase is completely soluble in the aqua regia, as all of the chromium was measured in the ICP-MS analysis. Furthermore, Cr content measured by XRF in spheres cooled down in argon showed lower Cr content than those cooled down in H_2/N_2, suggesting a small Cr loss, however not as significant as those observed with the ICP-MS measurements.

5.3. Mechanism of reaction using heating profile B

With the data collected in Tables 3-5 and the XRD patterns (Figure 4 and 7), a mechanism was proposed for the different reactions occurring during the synthesis of Cr doped uranium nitrides and is graphically shown in Figure 10.

1. The UO2+x is reduced to UO2 at temperatures below 1273 K. Afterwards, the chromia reacts and transforms into CrN at temperatures above 1373 K [27].

$$UO_{2+x} + xC \rightarrow UO_2 + xCO \tag{1}$$

$$Cr_2O_3 + 3C + N_2 \rightarrow CrN + 3CO \tag{2}$$

2. Between 1473-1773 K the chromium is decomposed into metallic Cr [25] and at the same time uranium is nitrided into UN.

$$2\ CrN \rightarrow 2\ Cr + N_2 \tag{3}$$

$$2UO_2 + 4\ C + N_2 \rightarrow 2UN + 4\ CO \tag{4}$$

3. Once the temperature starts to decrease, two different situations can happen:
   a. If the atmosphere is not changed, the nitrogen excess allows the formation of U2N3 and/or CrN, either of which can allow the stoichiometry of the reaction to be fulfilled. As the temperature keeps lowering, the remaining UN is transformed into U2N3 and UN2.

$$U_2N_3 + Cr \rightarrow U_2CrN_3 \tag{5}$$

$$2UN + CrN \rightarrow U_2CrN_3 \tag{6}$$

   b. If the atmosphere is changed to Ar, the metallic Cr cannot react with the UN that was formed, as nitrogen is missing for balancing the reaction. The chromium is then left as metallic chromium, which precipitates as a separate phase.

$$2UN + Cr \rightarrow U_2CrN_3 \tag{7}$$

5.4. Production of UN combined with U_2CrN_3

Sample UCrN-1 was denitrided at 1473 K in an argon atmosphere. The $UN_{1.5+x}$ phase is completely transformed into the UN after the treatment, and more importantly the ternary phase (U_2CrN_3) remained unaffected in the samples (Figure 8). Rietveld refinement showed that the ternary phase composition for sample UCrN-1 before denitridation was 20.8 %. The small increase to 21.5 % in ternary phase after denitridation is associated to the lower weight of UN compared to $UN_{1.5+x}$. These results also suggest that

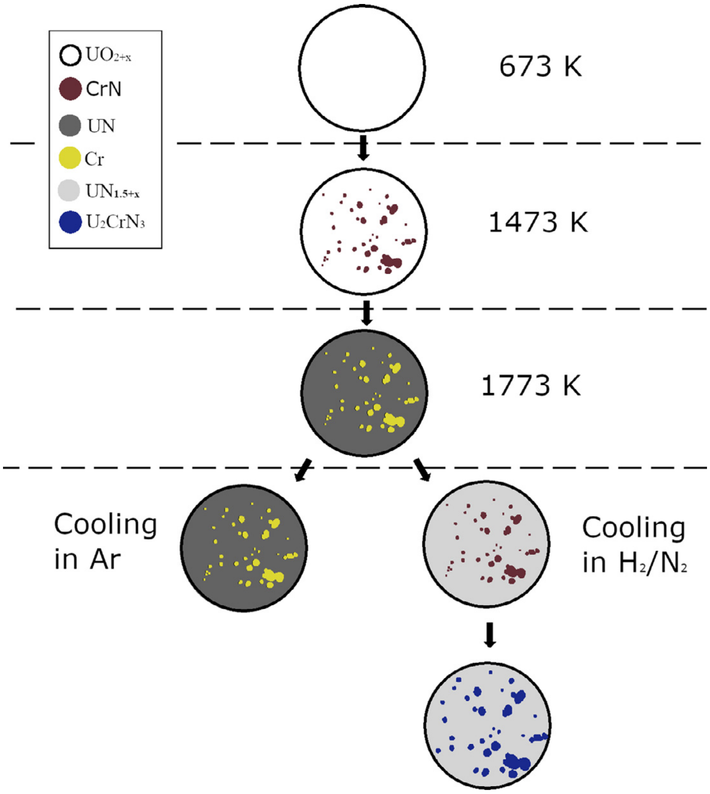

Figure 10. Proposed mechanism for the difference observed in materials when cooled down in argon or in H_2/N_2.

once the ternary phase is formed, it is stable up to 1473 K, which is expected from the calculations made by other authors [13,18].

After denitridation, patches of ternary phase were observed on the surface of the spheres (Figure 9). These patches appear to fuse with the UN phase, unlike the pebble like precipitates in the samples cooled down in argon (Figure 6). This phase was mainly located close to cracks in the spheres.

6. Conclusions

In this work the production of chromium doped uranium nitride via the sol-gel and carbothermic reduction was studied. Two different types of chromium doped materials were produced depending on the heating treatment.

It was observed that if the cooling gas was changed to an inert atmosphere such as argon, the material produced was pure UN with chromium precipitations. If the cooling gas was not changed, the ternary phase was formed in the materials, with the disadvantage of the formation of hyperstoichiometric nitrides. Posterior denitridation was achieved at 1473 K, showing that the ternary phase is stable up to this temperature.

A mechanism for the reactions occurring during the heating process was proposed. At high temperatures Cr is found as a metallic Cr. If the gas used during cool down is H_2/N_2, species rich in nitrogen are formed, which then are able to react and form the mixed U_2CrN_3 phase.

The main contaminants of the final products are carbon and oxygen as expected for the carbothermic reduction. Their content was reduced at higher temperatures or if the cooling gas was not changed. Chromium losses were measured using ICP-MS; on the other hand, XRF measurements showed that Cr losses were minimal. It was concluded that the chromium in the Cr-rich phase is insoluble in the aqua regia. On the other hand, chromium in the ternary phase was completely soluble in aqua regia.

Declaration of Competing Interest

The authors declare that they have no known competing financial interests or personal relationships that could have appeared to influence the work reported in this paper.

CRediT authorship contribution statement

L.G. Gonzalez Fonseca: Conceptualization, Methodology, Validation, Formal analysis, Investigation, Resources, Writing – original draft, Visualization. **J. Král:** Validation, Formal analysis, Investigation, Visualization. **M. Hedberg:** Conceptualization, Supervision, Writing – review & editing, Supervision. **T. Retegan Vollmer:** Supervision, Writing – review & editing.

Data availability

Data will be made available on request.

Acknowledgments

This research was financially supported by the Swedish Foundation for Strategic Research (SSF), project number EM16-0031. The authors wish to thank the Chalmers Materials Analysis Laboratory (CMAL) for their support during the SEM analysis. Additional thanks to Dr. Maria Lagerström from the Mechanics and Maritime Sciences department for their help with the XRF instrument.

References

[1] D.J. Park, H.G. Kim, Y. Il Jung, J.H. Park, J.H. Yang, Y.H. Koo, Behavior of an improved Zr fuel cladding with oxidation resistant coating under loss-of-coolant accident conditions, J. Nucl. Mater. 482 (2016) 75–82, doi:10.1016/j.jnucmat.2016.10.021.

[2] A. Naceur, G. Marleau, Neutronic analysis for accident tolerant cladding candidates in CANDU-6 reactors, Ann. Nucl. Energy. 113 (2018) 147–161, doi:10.1016/J.ANUCENE.2017.11.016.

[3] G.J. Youinou, R.S. Sen, Impact of Accident-Tolerant Fuels and Claddings on the Overall Fuel Cycle: A Preliminary Systems Analysis, Nucl. Technol. 188 (2014) 123–138, doi:10.13182/NT14-22.

[4] K.Y. Spencer, L. Sudderth, R.A. Brito, J.A. Evans, C.S. Hart, A. Hu, A. Jati, K. Stern, S.M. McDeavitt, Sensitivity study for accident tolerant fuels: Property comparisons and behavior simulations in a simplified PWR to enable ATF development and design, Nucl. Eng. Des. 309 (2016) 197–212, doi:10.1016/j.nucengdes.2016.09.009.

[5] P.E. Evans, T.J. Davies, Uranium nitrides, J. Nucl. Mater. 10 (1963) 43–55, doi:10.1016/0022-3115(63)90115-6.

[6] G.A.R. Rao, S.K. Mukerjee, V.N. Vaidya, V. Venugopal, D.D. Sood, Oxidation and hydrolysis kinetic studies on UN, J. Nucl. Mater. 185 (1991) 231–241, doi:10.1016/0022-3115(91)90340-D.

[7] K. Johnson, V. Ström, J. Wallenius, D.A. Lopes, Oxidation of accident tolerant fuel candidates, J. Nucl. Sci. Technol. 54 (2017) 280–286, doi:10.1080/00223131.2016.1262297.

[8] M. Jolkkonen, P. Malkki, K. Johnson, J. Wallenius, Uranium nitride fuels in superheated steam, J. Nucl. Sci. Technol. 54 (2017) 513–519, doi:10.1080/00223131.2017.1291372.

[9] B. Szpunar, L. Malakkal, S. Chung, M. Mateen Butt, E. Jossou, J.A. Szpunar, Accident tolerant composite nuclear fuels, MATEC Web Conf., 2017, doi:10.1051/matecconf/201713003001.

[10] D.R. Costa, M. Hedberg, S.C. Middleburgh, J. Wallenius, P. Olsson, D.A. Lopes, UN microspheres embedded in UO2 matrix: An innovative accident tolerant fuel, J. Nucl. Mater. 540 (2020) 152355, doi:10.1016/J.JNUCMAT.2020.152355.

[11] L.H. Ortega, B.J. Blamer, J.A. Evans, S.M. McDeavitt, Development of an accident-tolerant fuel composite from uranium mononitride (UN) and uranium sesquisilicide (U3Si2) with increased uranium loading, J. Nucl. Mater. 471 (2016) 116–121, doi:10.1016/j.jnucmat.2016.01.014.

[12] A. Prahlad Telles, A. Celeste White, J. Taylor, Report on Waterproofing of UN studies, 2019.

[13] Y. Mishchenko, K.D. Johnson, J. Wallenius, D.A. Lopes, Design and fabrication of UN composites: From first principles to pellet production, J. Nucl. Mater. 553 (2021) 153047, doi:10.1016/J.JNUCMAT.2021.153047.

[14] A. Herman, C. Ekberg, A uranium nitride doped with chromium, Nickel Aluminum Accid. Tolerant Fuel 5 (2017), doi:10.4172/2321-6212.1000196.

[15] K. Yang, E. Kardoulaki, D. Zhao, B. Gong, A. Broussard, K. Metzger, J.T. White, M.R. Sivack, K.J. Mcclellan, E.J. Lahoda, J. Lian, Cr-incorporated uranium nitride composite fuels with enhanced mechanical performance and oxidation resistance, J. Nucl. Mater. 559 (2022) 153486, doi:10.1016/J.JNUCMAT.2021.153486.

[16] R.B. Matthews, K.M. Chidester, C.W. Hoth, R.E. Mason, R.L. Petty, Fabrication and testing of uranium nitride fuel for space power reactors, J. Nucl. Mater. 151 (1988) 334–344.

[17] G.W.C. Silva, C.B. Yeamans, A.P. Sattelberger, T. Hartmann, G.S. Cerefice, K.R. Czerwinski, Reaction sequence and kinetics of uranium nitride decomposition, Inorg. Chem. 48 (2009) 10635–10642, doi:10.1021/IC901165J/ASSET/IMAGES/LARGE/IC-2009-01165J_0005.JPEG.

[18] H. Holleck, Ternary phase equilibria in the systems actinide-transition metal-carbon and actinide-transition metal-nitrogen, Thermodyn. Nucl. Mater., 1975 https://www.osti.gov/biblio/4177518.

[19] R. Benz, W.H. Zachariasen, Crystal structures of Th2CrN3, Th2MnN3, U2CrN3 and U2MnN3, J. Nucl. Mater. 37 (1970) 109–113, doi:10.1016/0022-3115(70)90187-X.

[20] S.M. Fatemi, M. Foroutan, Study of dispersion of carbon nanotubes by Triton X-100 surfactant using molecular dynamics simulation, J. Iran. Chem. Soc. 12 (2015) 1905–1913, doi:10.1007/s13738-015-0665-1.

[21] L.G. Gonzalez Fonseca, M. Hedberg, L. Huan, P. Olsson, T. Retegan Vollmer, Application of SPS in the fabrication of UN and (U,Th)N pellets from microspheres, J. Nucl. Mater. 536 (2020) 152181, doi:10.1016/j.jnucmat.2020.152181.

[22] H. Falk-Windisch, J.E. Svensson, J. Froitzheim, The effect of temperature on chromium vaporization and oxide scale growth on interconnect steels for solid oxide fuel cells, J. Power Sources. 287 (2015) 25–35, doi:10.1016/J.JPOWSOUR.2015.04.040.

[23] T. Sand, C. Geers, Y. Cao, J.E. Svensson, L.G. Johansson, Effective reduction of Chromium-oxy-hydroxide Evaporation from Ni-Base alloy 690, Oxid. Met. 92 (2019) 259–279, doi:10.1007/s11085-019-09935-9.

[24] V. Peres, L. Favergeon, M. Andrieu, J.C. Palussire, J. Balland, C. Delafoy, M. Pijolat, High temperature chromium volatilization from Cr2O3 powder and Cr2O3-doped UO2 pellets in reducing atmospheres, J. Nucl. Mater. 423 (2012) 93–101, doi:10.1016/J.JNUCMAT.2012.01.001.

[25] W. Ernst, J. Neidhardt, H. Willmann, B. Sartory, P.H. Mayrhofer, C. Mitterer, Thermal decomposition routes of CrN hard coatings synthesized by reactive arc evaporation and magnetron sputtering, Thin Solid Films 517 (2008) 568–574, doi:10.1016/J.TSF.2008.06.086.

[26] E.A. Gulbransen, K.F. Andrew, A preliminary study of the oxidation and vapor pressure of chromium, J. Electrochem. Soc. 99 (1952) 402.

[27] S. Morita, H. Shimizu, Y. Sayama, Synthesis of chromium nitride powder by carbo-thermal nitriding, in: 15th Int. Plansee Semin., Plansee Holding AG, 2001, pp. 139–154.

[28] D. Mukherji, M. Klauke, P. Strunz, I. Zizak, G. Schumacher, A. Wiedenmann, J. Rösler, High temperature stability of Cr-carbides in an experimental Co-Re-based alloy, Int. J. Mater. Res. 101 (2010) 340–348, doi:10.3139/146.110282/MACHINEREADABLECITATION/RIS.

[29] G.B. Reartes, P.J. Morando, M.A. Blesa, P.B. Hewlett, E. Matijević, Reactivity of chromium oxide in aqueous solutions. 2. Acid dissolution, Langmuir 11 (1995) 2277–2284, doi:10.1021/LA00006A068/ASSET/LA00006A068.FP.PNG_V03.